RESEARCH PAPER

Epigenetics 9:4, 611–620; April 2014; © 2014 Landes Bioscience

BET bromodomain proteins are required for glioblastoma cell proliferation

Chiara Pastori[1,†], Mark Daniel[1,†], Clara Penas[1], Claude-Henry Volmar[1], Andrea L Johnstone[1], Shaun P Brothers[1], Regina M Graham[2], Bryce Allen[1], Jann N Sarkaria[3], Ricardo J Komotar[2], Claes Wahlestedt[1], and Nagi G Ayad[1,*]

[1]Center For Therapeutic Innovation; Department of Psychiatry and Behavioral Sciences; University of Miami Miller School of Medicine; Miami, FL USA; [2]Department of Neurosurgery; University of Miami Miller School of Medicine; Miami, FL USA; [3]Department of Radiation Oncology; Mayo Clinic; Rochester, MN USA

[†]These authors contributed equally to this work.

Keywords: glioblastoma, epigenetics, bromodomain, stem cells, histones, histone acetylation mimics, temozolomide

Abbreviations: GBM, glioblastoma; BET, bromodomain and extra terminal domain; TMZ, temozolomide

Epigenetic proteins have recently emerged as novel anticancer targets. Among these, bromodomain and extra terminal domain (BET) proteins recognize lysine-acetylated histones, thereby regulating gene expression. Newly described small molecules that inhibit BET proteins BRD2, BRD3, and BRD4 reduce proliferation of NUT (nuclear protein in testis)-midline carcinoma, multiple myeloma, and leukemia cells in vitro and in vivo. These findings prompted us to determine whether BET proteins may be therapeutic targets in the most common primary adult brain tumor, glioblastoma (GBM). We performed NanoString analysis of GBM tumor samples and controls to identify novel therapeutic targets. Several cell proliferation assays of GBM cell lines and stem cells were used to analyze the efficacy of the drug I-BET151 relative to temozolomide (TMZ) or cell cycle inhibitors. Lastly, we performed xenograft experiments to determine the efficacy of I-BET151 in vivo. We demonstrate that *BRD2* and *BRD4* RNA are significantly overexpressed in GBM, suggesting that BET protein inhibition may be an effective means of reducing GBM cell proliferation. Disruption of *BRD4* expression in glioblastoma cells reduced cell cycle progression. Similarly, treatment with the BET protein inhibitor I-BET151 reduced GBM cell proliferation in vitro and in vivo. I-BET151 treatment enriched cells at the G1/S cell cycle transition. Importantly, I-BET151 is as potent at inhibiting GBM cell proliferation as TMZ, the current chemotherapy treatment administered to GBM patients. Since I-BET151 inhibits GBM cell proliferation by arresting cell cycle progression, we propose that BET protein inhibition may be a viable therapeutic option for GBM patients suffering from TMZ resistant tumors.

Introduction

Epigenetic signaling pathways regulate gene expression without altering DNA sequences.[1,2] This is achieved, in part, by adding acetyl groups to lysine residues on histones H2A, H2B, H3, and H4, thereby modulating chromatin structure and gene expression.[1,2] Histone acetyltransferases (HATs) attach acetyl groups to histones while histone deacetylases (HDACs) remove acetyl moieties.[1,2] Coupled to HAT and HDAC activity, bromodomain reader proteins bind acetylated histones and recruit transcriptional complexes, therefore representing an important link between histones and transcription.[1,2] Among the 46 known bromodomain proteins, the bromodomain and extra terminal domain (BET) proteins BRD2, BRD3, BRDT, and BRD4 bind the super elongation complex (SEC) and the polymerase associated factor complex (PAFc) in certain biological contexts.[3] In addition, BRD4 recruits the positive transcription elongation complex P-TEFb.[4,5] Several recent studies have uncovered roles for the BET proteins by designing small molecules that act as histone mimics, thereby displacing BET proteins from acetylated histones and the transcriptional machinery.[3,6-10] BET protein displacement from chromatin is associated with decreases in transcription of lipopolysaccharide (LPS)-inducible genes and oncogenes, and is therefore attractive therapeutically for the treatment of inflammation or cancer.[1,2] Small molecules that antagonize BET protein binding to acetylated histones have shown efficacy in mouse models of inflammation, NUT-midline carcinoma, mixed lineage leukemia (MLL) fusion, multiple myeloma, high-risk acute lymphoblastic leukemia, and lung adenocarcinoma.[3,6-9,11,12] These small molecules (JQ1, GSK525762A [I-BET] and I-BET151) exhibit remarkable specificity for the BET bromodomain proteins BRD2, BRD3, BRD4, and BRDT over other bromodomain proteins and epigenetic enzymes.[3,6-9,11] Consistent with this specificity, GSK525762A is currently being tested in clinical trials for the treatment of NUT-midline carcinoma (NCT01587703). Collectively, these studies suggest that BET bromodomain small molecule antagonists may be effective in treating aggressive cancers.

*Correspondence to: Nagi G Ayad; Email: nayad@med.miami.edu
Submitted: 09/18/2013; Revised: 01/10/2014; Accepted: 01/17/2014; Published Online: 02/19/2014
http://dx.doi.org/10.4161/epi.27906

BET protein inhibition might be a possible therapy against the most common primary adult brain cancer, glioblastoma (GBM).[13,14] Prognosis for GBM patients is poor with median survival of approximately 13 mo for those patients who had complete surgical resection, and even lower for those where surgery is contraindicated.[13,14] Current treatment regimens include radiotherapy in combination with the DNA alkylating agent temozolomide (TMZ).[13,14] However, TMZ resistance is nearly universal, and therefore novel small molecule inhibitors of GBM cell proliferation are needed.[13,14] Further, recent studies have demonstrated that GBM stem cells are resistant to TMZ therapy and promote tumor recurrence[15] and, therefore, small molecules that effectively eliminate GBM stem cells are highly desirable.

We demonstrate that small molecule inhibitors of BET proteins are possible therapies for GBM patients since they inhibit proliferation of GBM cells. Treatment of GBM cells with I-BET151 potently inhibits proliferation. I-BET151 treatment arrested U87MG cells in G1/S, thus providing mechanistic insight into how I-BET151 may reduce cell proliferation in vivo. I-BET151 treatment also inhibits growth of U87MG xenografts in immunocompromised mice, suggesting that I-BET151 analogs that cross the blood brain barrier may be effective as single agents or in combination therapy for GBM treatment.

Results

BRD2 and BRD4 are significantly elevated in glioblastoma tumors

To identify possible therapeutic targets in GBM, we used NanoString Technology to determine the expression of 40 bromodomain proteins in 27 GBM tumors relative to 9 control samples isolated from epilepsy patients. We utilized the NanoString nCounter system to assess gene expression quantitatively.[16] As shown in **Figure 1A–C and Table 1**, the RNA levels of ten bromodomain-containing proteins were differentially expressed in GBM tumors as determined by Bonferroni corrected *P* values. Because Bonferroni multiple comparison correction can often result in false negatives, a Benjamini-Hochberg multiple comparisons correction was also used to identify significant genes, using a stringent false discovery rate (FDR) of 1%.[17]

Genes exhibiting significant expression changes tended to cluster together based on sequence similarity (**Fig. 1C**). Two members of the BET family of bromodomains, *BRD2* and *BRD4*, were significantly increased in glioblastoma, as their expression was 1.8-fold higher in GBM samples relative to control. Further, when the BRD proteins were ranked by *P* value, *BRD4* was the third most significantly elevated RNA relative to all other RNAs encoding bromodomain proteins (**Fig. 1A and B**; **Table 1**). Collectively, these studies suggested that BRD2 and BRD4 might be attractive therapeutic targets since they are elevated in GBM tumors relative to control tissue.

BET bromodomain protein inhibition reduces glioblastoma cell proliferation

Since *BRD4* was elevated in GBM tumors relative to controls and has been implicated in promoting proliferation of multiple cancer cell lines, we asked whether disrupting its activity affected U87MG cell proliferation. We reduced *BRD4* expression utilizing a well-characterized siRNA and measured *BRD4* mRNA levels via qRT-PCR analysis. As seen in **Figure 2A**, *BRD4* mRNA levels were significantly decreased in cells transfected with siRNA targeting *BRD4* relative to control siRNA-transfected cells ($P < 0.001$). *BRD4* siRNA treated cells contained lower cellular ATP ($P < 0.001$) as measured by a Cell-Titer-Glo Assay (**Fig. 2B**). Further, U87MG cells containing lower *BRD4* proliferated less than control-transfected cells ($P < 0.001$), as measured by an EdU incorporation assay (**Fig. 2C**).

To determine whether pharmacological inhibition of BRD2, BRD3, and BRD4 similarly reduced U87MG ATP levels and cell proliferation, we utilized the small molecule inhibitor I-BET151. I-BET151 treatment dose-dependently reduced cellular levels of ATP as measured by a CellTiter-Glo assay (**Fig. 3A and B**). The mean IC_{50} value for I-BET151 in a CellTiter-Glo assay was 1.05 ± 0.18 μM at 48 h and 0.572 ± 0.048 μM at 72 h (**Fig. 3A and B**). Slightly higher IC_{50} values were observed for I-BET151 on glioblastoma cell lines A172 and SW1783 as well as patient derived glioblastoma stem cells (approximately 1.28 ± 0.23 μM, 2.68 ± 0.45 μM, and 1.12 ± 0.23 μM, respectively, **Figs. S1 and S2**). Further, I-BET151 was as potent as TMZ and different cell cycle inhibitors in reducing cellular ATP levels in U87MG cells (**Fig. S1**). The reduction in ATP levels was accompanied by inhibition of cell proliferation since I-BET151 treatment reduced EdU incorporation in U87MG and Patient-derived cells (**Fig. 3C and D**; **Fig. S7**).

Since I-BET151 treatment reduced proliferation of U87MG cells, we tested whether it affected cell cycle transition. To test this directly, we performed propidium iodide analysis (PI-FACS) and found that I-BET151 treatment increased the number of U87MG cells in the G1 phase of the cell cycle. I-BET151 treated cells also contained lower percentage of S phase cells, suggesting that BET bromodomain proteins control G1 progression (**Fig. 4**).

BET bromodomain protein control of cell cycle progression may reduce U87MG cell cycle transit from G1 to S phase given the increased number of G1 cells observed after I-BET151 treatment. To test this directly, we performed FUCCI live cell imaging analysis of U87MG cells in the presence of I-BET151 or DMSO control. The FUCCI system has been utilized to measure cell cycle progression in vitro and in vivo.[18] It utilizes fluorescent degradation reporters, which mark G1 (red), S/G2/M (green), or the G1/S transition (yellow). As shown in **Figure 5A and B**, treatment of U87GM cells with I-BET151 increased the number of G1/S (yellow) cells relative to control over time. By contrast, the percentage of S/G2/M (green) cells decreased upon I-BET151 treatment (**Fig. 5A and B**; **Fig. S3**). Collectively, these studies suggest that I-BET151 treatment arrests cells at the G1/S transition.

I-BET151 treatment reduces tumor size of U87MG xenografts

I-BET151 inhibition of cell proliferation in U87MG cells suggests that it may be an effective means of inhibiting GBM tumor growth in vivo. To test this directly, we injected immunocompromised mice subcutaneously with U87MG

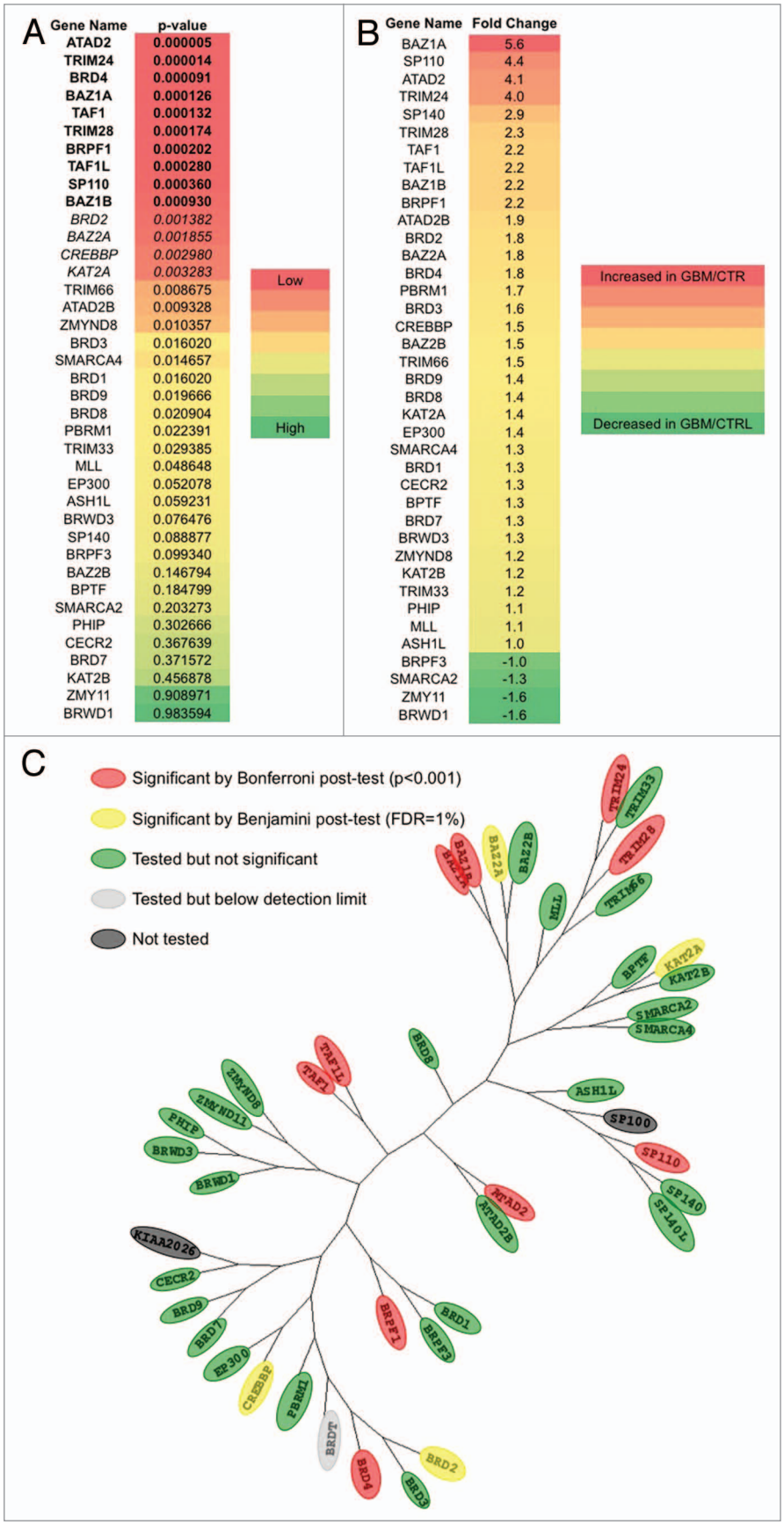

Figure 1. *BRD2* and *BRD4* are elevated in Glioblastoma. A. Heat maps of genes elevated in GBM tumors ranked by *P* values. Genes with $P < 0.001$ (Bonferroni correction) are shown in bold. In italics are genes that pass a Benjamini-Hochberg post-test with a false discovery threshold of 1%. (**B**) Heat map of genes elevated in GBM ranked by fold change. (**C**) Phylogenetic Tree of Bromodomain Proteins. A gene-based phylogenetic tree was constructed using ChromoHub (Structural Genomics Consortium[30]). Genes on the tree were color-coded according to level of significance between glioblastoma and control expression levels. The most significant genes were those that passed a *t* test with Bonferroni multiple comparisons correction ($P < 0.001$, green). Genes that passed a less stringent Benjamini-Hochberg post-test (allowing for a false discovery rate, or FDR, of 1%) are highlighted in yellow.

cells followed by I-BET151 (10 mg/kg; i.p. daily) or saline injection. As shown in **Figure 6**, saline injected animals had much larger tumors than the I-BET151 injected counterparts ($P < 0.05$), suggesting that I-BET151 reduced proliferation of U87MG cells in vivo. Importantly, I-BET151 was as effective as TMZ at inhibiting tumor growth in vivo. Further, I-BET151 appears to be well tolerated by animals, since no difference in weight was observed in saline or I-BET151 treated mice (**Fig. S4**).

Discussion

Our studies identified the BET bromodomain proteins as possible therapeutic targets in GBM. We demonstrated that the BET bromodomain proteins BRD2 and BRD4 are significantly elevated in GBM tumors relative to controls. Based on these findings, we tested whether siRNA mediated depletion of *BRD4* in U87MG cells significantly reduced proliferation. *BRD4* depletion reduced U87MG cell proliferation as measured by an EdU incorporation assay. Similarly, treatment with the BET bromodomain inhibitor I-BET151 reduced EdU incorporation in U87MG cells, suggesting the I-BET151 effects on cell proliferation are at least partly mediated through BRD4 inhibition. I-BET151 treatment arrests U87MG cells at the G1/S transition as revealed by FACS and FUCCI analysis. These in vitro studies suggested that I-BET151 treatment might be a possible means of reducing GBM cell proliferation in vivo. Indeed, I-BET151

Table 1. Relative Expression of Bromodomain Proteins in glioblastoma (GBM) and control (CTR) samples

Gene name	Accession Number	GBM mean expression	CTR mean expression	Fold change (GBM/CTR)	*P* value	Bonferroni corrected *P* < 0.001?	Benjamini *P* < FDR?
ATAD2	**NM_014109.3**	**274.4**	**67.5**	**4.1**	**0.000005**	**YES**	**YES**
TRIM24	**NM_015905.2**	**494.5**	**123.3**	**4.0**	**0.000014**	**YES**	**YES**
BRD4	**NM_014299.2**	**912.7**	**514.1**	**1.8**	**0.000091**	**YES**	**YES**
BAZ1A	**NM_182648.1**	**223.3**	**39.6**	**5.6**	**0.000126**	**YES**	**YES**
TAF1	**NM_004606.2**	**169.8**	**77.1**	**2.2**	**0.000132**	**YES**	**YES**
TRIM28	**NM_005762.2**	**1216.2**	**517.8**	**2.3**	**0.000174**	**YES**	**YES**
BRPF1	**NM_001003694.1**	**193.5**	**88.8**	**2.2**	**0.000202**	**YES**	**YES**
TAF1L	**NM_153809.1**	**207.0**	**94.1**	**2.2**	**0.000280**	**YES**	**YES**
SP110	**NM_004510.3**	**290.5**	**65.8**	**4.4**	**0.000360**	**YES**	**YES**
BAZ1B	**NM_032408.3**	**846.0**	**384.8**	**2.2**	**0.000930**	**YES**	**YES**
BRD2	*NM_001113182.1*	*1270.1*	*697.7*	*1.8*	*0.001382*	*NO*	*YES*
BAZ2A	*NM_013449.3*	*225.0*	*125.1*	*1.8*	*0.001855*	*NO*	*YES*
CREBBP	*NM_001079846.1*	*320.2*	*207.5*	*1.5*	*0.002980*	*NO*	*YES*
KAT2A	*NM_021078.2*	*376.4*	*269.7*	*1.4*	*0.003283*	*NO*	*YES*
TRIM66	NM_014818.1	62.5	42.5	1.5	0.008675	NO	NO
ATAD2B	NM_001242338.1	192.3	99.5	1.9	0.009328	NO	NO
ZMYND8	NM_012408.3	258.5	214.2	1.2	0.010357	NO	NO
BRD3	NM_007371.3	250.4	154.8	1.6	0.010383	NO	NO
SMARCA4	NM_003072.3	551.4	421.8	1.3	0.014657	NO	NO
BRD1	NM_014577.1	138.1	106.2	1.3	0.016020	NO	NO
BRD9	NM_001009877.2	347.7	243.5	1.4	0.019666	NO	NO
BRD8	NM_001164326.1	639.1	452.5	1.4	0.020904	NO	NO
PBRM1	NM_181042.3	247.9	148.1	1.7	0.022391	NO	NO
TRIM33	NM_015906.3	383.5	333.6	1.2	0.029385	NO	NO
MLL	NM_005933.3	271.8	256.7	1.1	0.048648	NO	NO
EP300	NM_001429.2	295.9	216.1	1.4	0.052078	NO	NO
ASH1L	NM_018489.2	503.0	481.5	1.0	0.059231	NO	NO
BRWD3	NM_153252.4	317.0	249.8	1.3	0.076476	NO	NO
SP140	NM_001005176.2	46.1	16.1	2.9	0.088877	NO	NO
BRDT*	NM_001726.3	1.9	1.3	1.4	0.091369	NO	NO
BRPF3	NM_015695.2	95.7	99.5	-1.0	0.099340	NO	NO
BAZ2B	NM_013450.2	454.3	308.3	1.5	0.146794	NO	NO
BPTF	NM_182641.3	450.9	351.5	1.3	0.184799	NO	NO
SMARCA2	NM_003070.3	747.7	955.0	-1.3	0.203273	NO	NO
PHIP	NM_017934.5	481.7	426.0	1.1	0.302666	NO	NO
CECR2	NM_031413.3	64.9	50.2	1.3	0.367639	NO	NO
BRD7	NM_001173984.2	470.9	368.7	1.3	0.371572	NO	NO
KAT2B	NM_003884.3	525.8	438.0	1.2	0.456878	NO	NO
ZMY11	NM_001202464.1	544.5	861.2	-1.6	0.908971	NO	NO
BRWD1	NM_001007246.2	516.6	835.2	-1.6	0.983594	NO	NO

Genes with P < 0.001 (Bonferroni correction) are shown in bold. In italics are genes that passed a Benjamini-Hochberg post-test with a false discovery threshold of 1%. Asterisk next to the gene name indicates that gene was below the threshold for background, and was therefore deemed to be undetected in the samples.

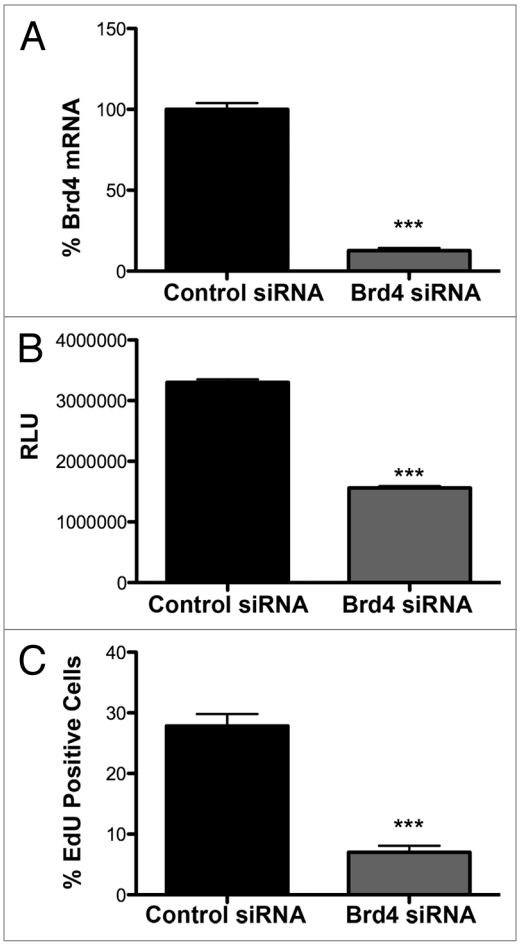

Figure 2. *BRD4* knockdown reduces U87MG cell proliferation. (**A**) *BRD4* RNA levels are reduced after siRNA transfection of U87MG cells U87MG cells were transfected twice with 50 nM *BRD4* siRNA or control. Five days after transfection, RNA was extracted and used to verify the knockdown efficiency with quantitative RT-PCR. *BRD4* RNA levels were normalized relative to the Actin housekeeping gene. (**B**) Cells transfected with *BRD4* siRNA have less cellular ATP than control-transfected cells as measured by a CellTiter-Glo assay. Half of the cells transfected with Brd4 siRNA in A were analyzed for ATP content using the CellTiter-Glo Assay. RLU, Relative Luminescence Levels (**C**) Cells transfected with *BRD4* siRNA proliferate less than control siRNA transfected cells as measured by an EdU incorporation assay (***$P < 0.001$ by the Student t test; n = 3). Results shown are from three independent experiments.

treatment of immunocompromised mice sharply inhibited tumor growth in a flank mouse model.

Further studies are required to identify the I-BET151 target(s) responsible for growth inhibition in vivo. I-BET151 has been shown to inhibit BRD2, BRD3, and BRD4 activity.[3,19,20] We have shown that *BRD4* depletion reduces U87MG cell proliferation and thus is one of the likely targets affected by I-BET151 in vitro and in vivo. BRD2 has an established cell cycle role[10,20,21] and a recent study found that depletion of either *BRD2* or *BRD4* but not *BRD3* reduces glioblastoma cell proliferation.[22] We compared the effects of *BRD3* and *BRD2* knockdown to *BRD4* depletion and we confirmed that *BRD3* is not essential for U87MG proliferation (**Fig. S8**). However, further studies are required to determine the relative contribution of *BRD2* and *BRD4* to GBM cell proliferation since these two proteins are likely to have overlapping or independent functions and targets in proliferation and inflammation.

Perhaps similar to what was performed for various kinases,[23,24] mouse models can be developed that harbor I-BET151 insensitive versions of *BRD2* or *BRD4* to fully validate these targets in GBM.

An alternative means of validating BRD2 and BRD4 as targets in GBM is the use of different chemical scaffolds, which inhibit BRD2 and BRD4 activity. Indeed, JQ1 contains a different chemical scaffold from I-BET151 and inhibits growth of GBM cells.[22] Since JQ1 is brain penetrant, it is an important tool compound for studying the role of BET bromodomain proteins in vivo.

It is unlikely that I-BET151 is brain penetrant and thus it is unclear if it can also be used for in vivo validation of BET bromodomain proteins as targets in GBM. However, based on its high polar surface area (93 A2), I-BET151 is less likely to be robustly brain penetrant, which is further supported by its low permeability and moderate efflux in MDCK-MDR1 cells (unpublished observations). Thus, chemical optimization is likely required to generate brain penetrant I-BET151 analogs.

It will be interesting to determine whether these I-BET151 analogs inhibit progression of GBM cell proliferation from G1 into S phase since our studies suggest this is a major means through which I-BET151 inhibits cell cycle progression. We find that I-BET151 induces accumulation of U87MG cells in G1 as revealed by FACS analysis. This is likely true for multiple BET bromodomain inhibitors since JQ1 induced G1 arrest in U87MG cells.[22] Our studies extend these findings to suggest that BET bromodomain inhibition induces accumulation of cells at the G1/S transition. FUCCI analysis revealed that U87MG cells treated with I-BET151 accumulate at G1/S. This was confirmed in HeLa cells, which arrested at G1/S upon I-BET151 treatment as revealed after synchronization and FACS analysis (unpublished observations). Thus, I-BET151 induction of G1/S arrest may be broadly applicable to multiple cell types where BET bromodomain proteins are required for entry into S phase from G1.

BET bromodomain control of the G1/S transition may be related to a newly discovered role for these proteins in transcriptional modulation at super enhancers.[25] BRD4 was found to be associated with super-enhancers that control expression of oncogenes required for multiple myeloma or GBM cell proliferation.[25] Interestingly, treatment with JQ1 reduced BRD4 binding to super enhancers within 6 h, which is within the time frame we began observing statistically significant differences between I-BET151 and DMSO treated cells by FUCCI analysis (**Fig. S3**). Future studies are required to determine whether the cell cycle inhibition we observe at G1/S is related to BET bromodomain proteins' role as transcriptional modulators at super-enhancers.

BET bromodomain protein control of super enhancers is thought to be cancer type dependent. For instance, JQ1 treatment reduced BRD4 occupancy at the *C-MYC* enhancer in multiple myeloma but not GBM cells.[25] This agrees with a recent

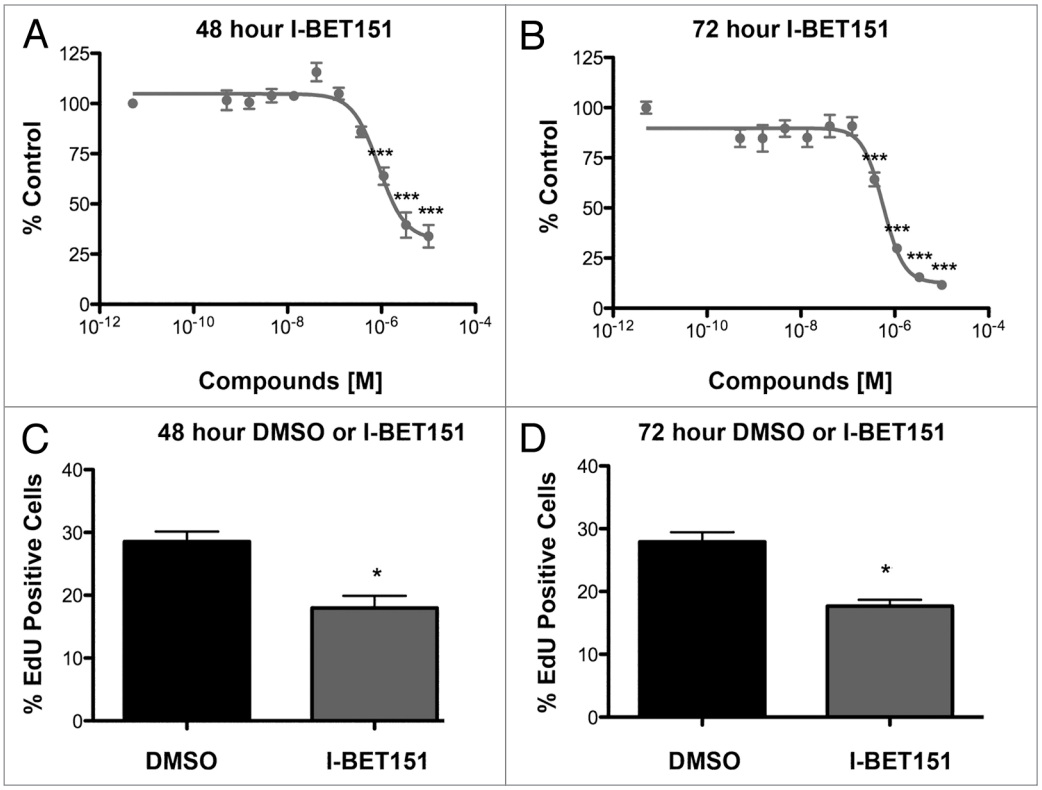

Figure 3. I-BET151 treatment reduces U87MG cellular ATP and proliferation in vitro. (**A**) IC_{50} of I-BET151 in a CellTiter-Glo assay. U87 cells treated for 48 h with the indicated doses of I-BET151. (**B**) IC_{50} of 72-h treatment of U87MG cells with I-BET151. (**C**) EdU incorporation assay of U87MG cells after 48-h treatment with I-BET151. (**D**) EdU incorporation assay of 72-h I-BET151 treatment of U87MG cells. 48 and 72 h CellTiter Glo, ***$P < 0.001$ by Bonferroni Post hoc comparison, n = 3, 48 and 72 h EdU assay, *$P < 0.05$ by the Student *t* test, n = 3. Results shown are from three independent experiments.

study where *C-MYC* levels were unchanged after JQ1 treatment of GBM cells.[22] Our studies suggest that *C-MYC* levels do not decrease after I-BET151 treatment (**Fig. S5A**). Thus, it does not appear that BET bromodomain proteins regulate *C-MYC* levels in GBM cells. Similarly, we did not observed upregulation of Hexim1, an inhibitory component of the positive transcription elongation factor b (P-TEFb) complex, which was increased after JQ1 in T cells.[26] To determine if it was similarly upregulated in GBM cells, we tested *Hexim1* expression after 24 h of I-BET151 treatment. However, we found significant downregulation of *Hexim1* after I-BET151 treatment (**Fig. S9D**). This may suggest that *Hexim1* is differentially regulated in GBM cells relative to T-cells.

To identify possible transcriptional targets of BET bromodomain proteins in GBM cells, we treated U87MG, A172, and GBM stem cells with either 500 nM I-BET151 or DMSO for 24 h and performed Affymetrix array analysis (**Fig. S5B**). As shown in Figures S5 and S6, some RNAs were significantly altered upon I-BET151 treatment. However, we were unable to find common RNAs that could be directly linked to GBM cell proliferation. Perhaps BET bromodomain proteins regulate a network of proteins involved in proliferation and only by performing mathematical modeling can we discover their role in controlling the G1/S transition.[27]

A recent study demonstrated that the RNA and protein levels of the cyclin-dependent-kinase inhibitor $p21^{Cip1}$ increase after JQ1 treatment.[22] Importantly, $p21^{Cip1}$ downregulation reduced growth inhibition after JQ1 treatment, suggesting that $p21^{Cip1}$ is an important downstream target of BET bromodomain proteins.[22] Consistent with these findings, we observed a significant increase of $p21^{Cip1}$ in both *mRNA* and protein after I-BET151 treatment (**Fig. S9A and B**). $p21^{Cip1}$ upregulation after BET bromodomain protein inhibition is consistent with our FACS and FUCCI analysis, which showed an increase of cells in G1 after I-BET151 treatment. $p21^{Cip1}$ protein levels are thought to be high during G1 to maintain low cyclin-dependent-kinase activity. During the G1/S transition, $p21^{Cip1}$ levels decrease to allow S phase entry. Thus, BET bromodomain proteins may reduce $p21^{Cip1}$ levels during late G1/S to promote S phase entry and cell cycle progression. By contrast, BET bromodomain inhibitors may induce $p21^{Cip1}$ levels, thus blocking cells at the G1/S transition. This model predicts that BET bromodomain inhibition is analogous to cyclin-dependent-kinase attenuation during the G1/S transition. It will be important to determine whether BET bromodomain inhibitors synergize with cyclin-dependent-kinase inhibitors in vitro and in vivo. We did not observe apoptosis after I-BET151 treatment. This may be due to the fact that we were concentrating on short treatments (24–72 h) and were mainly observing cell cycle arrest. Our FUCCI analysis visualized the cells for 24 h and we did not observe cell death within this time frame. This was also true for our PI-FACS analysis. However, after 72 h of treatment we began to observe reduction of an anti-apoptotic

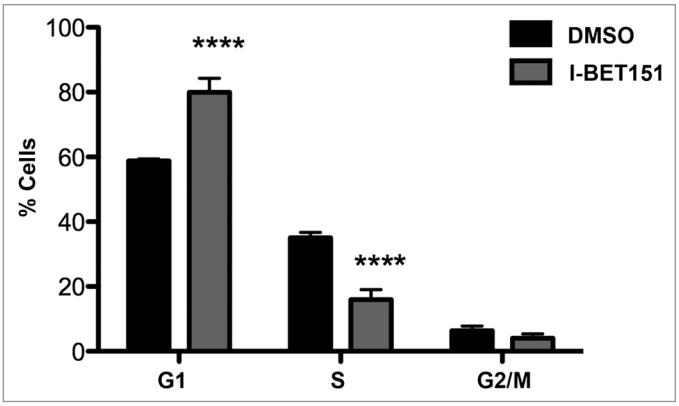

Figure 4. I-BET151 treatment increases G1 population of U87MG cells. PI-FACS analysis of U87MG cells treated with I-BET151 or DMSO control for the indicated times. Cell cycle phase was assessed by Flow-Jo analysis and represented as % total cells. ****$P < 0.0001$ by 2way ANOVA, n = 3. Results shown are from three independent experiments.

gene *BCL2*, which may eventually lead to apoptosis (**Fig. S9**). Finally, it will also be essential to determine whether patients who develop resistance to cyclin-dependent-kinase inhibitors are responsive to BET bromodomain inhibition. Future studies are required to fully explore the potential of bromodomain protein inhibition in combination therapies for the treatment of GBM.

Materials and Methods

Tissue specimen collection

Glioblastoma samples and relative controls (epilepsy) specimens were provided by the Florida Center for Brain Tumor Research (IRB project# 134-2006).

NanoString nCounter assay

Total RNA samples were submitted to the University of Miami Oncogenomics Core Facility for analysis using the NanoString nCounter gene expression system (Nanostring Technologies). Detailed methods for NanoString have been described elsewhere.[16] Briefly, two 100 base pair sequences complementary to each mRNA of interest were constructed. These probes consisted of one capture and one reporter probe specific to 40 human mRNA targets. The reaction was multiplexed so that all probes were simultaneously hybridized to 100 ng of total mRNA in one sample. The tripartite capture-reporter-target complexes were affinity purified and immobilized to a streptavidin-coated cartridge via a biotin tag on the capture probe. Each sample lane contained positive and negative controls to be used to adjust for systemic variability and to estimate non-specific background signal, respectively. A color-coded sequence unique to the reporter probe for each target RNA was read using an automated imager after elongation, alignment, and immobilization of the molecule using electrophoresis.

Data analysis was conducted using nSolver software (NanoString Technologies). To correct for systemic variability, each sample lane was normalized to the average signal of the positive spiked-in controls. To control for differences between sample input, each lane was then normalized to a reference

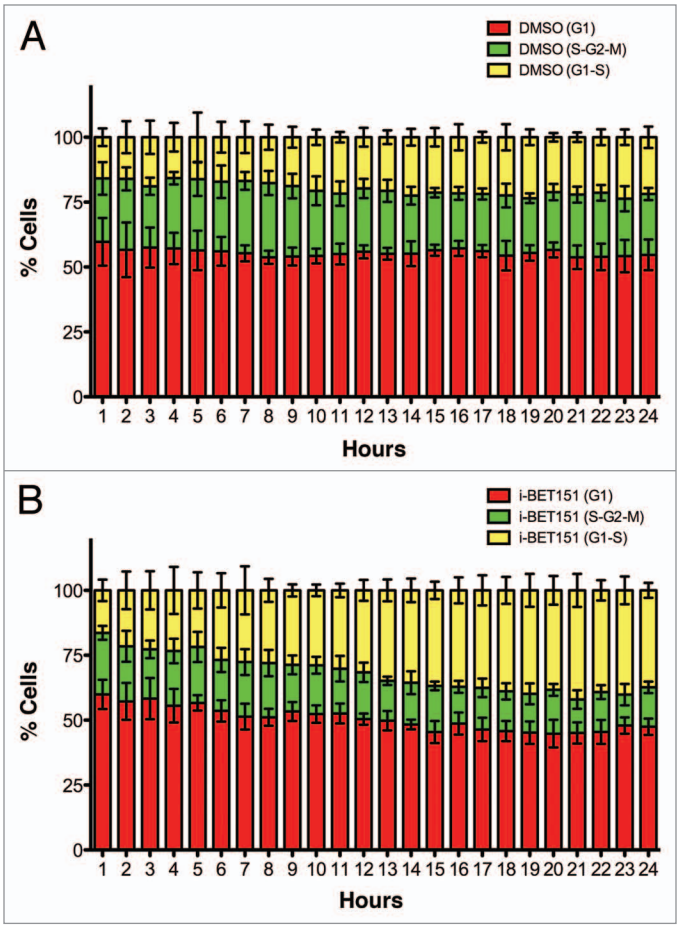

Figure 5. I-BET151 treatment increases proportion of cells in the G1/S transition. (**A**) Percentage of U87MG cells in G1, S/G2/M, or G1/S phases treated with DMSO. (**B**) Percentage of U87MG cells in G1, S/G2/M, or G1/S phases treated with I-BET151. FUCCI analysis was performed as described in Materials and Methods. Results are from three independent experiments. Statistical analysis described in **Figure S3**.

gene (SMYD3 was chosen based on stable expression between glioblastoma and control samples). Finally, to determine whether expression levels were above background noise, the mean of all the negative spiked-in controls was added to three times the standard deviation. Any target exhibiting a mean signal below this background threshold in both glioblastoma and control samples was considered to be undetected. A *t* test with Bonferroni corrected familywise error rate ($P < 0.001$) was used to identify genes with significant expression changes between control and glioblastoma samples. A Benjamini-Hochberg analysis was also used to identify significant genes, allowing for a false discovery rate of 1%.[17]

Cell lines

U87MG, A172, and SW1783 glioblastoma cell lines were purchased from ATCC and cultured in the recommended media at 37 °C and 5% CO_2. Patient's cell line UM20 was cultured in DMEM/F12 plus 5% FBS and non-essential amino acids (NEAA, Invitrogen). Patient's cancer stem cell lines Glio1 and Glio3 were cultured in DMEM/F12 (3:1) (Invitrogen) supplemented with 20 ng/ml EGF (Epidermal Growth Factor), 20 ng/ml bFGF

(basic Fibroblast Growth Factor), and 2% Gem21Neuroplex and 1% anti-mycotic/anti-biotic (Gemini Bio-Products).

GBM6 and GBM10 are primary GBM xenografts (PDX, Patient Derived Xenograft) established in the Sarkaria Laboratory (Mayo Clinic) by implanting patient tumors directly into the flank of nude mice. These xenograft lines are then maintained by serial transplantation in mice. These cells were cultured in vitro according to Carlson et al.[28]

ATP measurements

U87MG, A172, SW1783, patient tumor cells (UM20), and patient derived glioblastoma stem cells (Glio 1 and Glio3) were maintained in culture in 150-cm^2 flasks at 37 °C with 5% CO_2. The cells were seeded in white 384-well plates at a density of 5×10^2 cells per well in 25 μl medium. After the cells were allowed to attach and grow for 24 h, a 5 μl drug solution with different concentrations of I-BET151 or temozolomide (TMZ) was added to each well. In order to generate dose response curves, each cell type was treated in triplicate with test compounds, in a 10-point 1:3 dilution series starting at a nominal test concentration of 10 μM with the exception of TMZ, used at 100 μM. The cells were incubated for 48 to 72 h (depending on the compound treatment), followed by the CellTiter-GLo assay (Promega) for cell proliferation measurements. The Envision Multilabel Reader (Perkin Elmer) was used to measure the luminescent signal produced by the live cells.

For each compound tested, percent cell proliferation was plotted against compound concentration using the software GraphPad Prism (version 5.0c). The reported IC_{50} values were generated from fitted curves by solving for the X-intercept value at the 50% inhibition level of the Y-intercept value.

GraphPad Prism was also used to generate and analyze bar graphs. In cases where only two means were compared, data were analyzed with the two-tailed Student *t* test. For dose response curves, data were analyzed by ANOVA followed by Bonferroni Post hoc comparison of all the means to determine significance (***$P < 0.001$; **$P < 0.01$; *$P < 0.05$; n = 3).

EdU incorporation assays

U87MG, GBM6 and GBM10 cells were grown to a confluence of 50–60%. Then, I-BET151 (500 nM or 1 μM) or DMSO was added. After 24 or 48 h, EdU (20 nM) was added for 2 h and cells were fixed with 4% paraformaldehyde. Immunostaining for EdU and counterstaining with Hoechst was developed with the Click-iT® EdU Imaging Kit with Alexa Fluor 594 Azide (Invitrogen) following manufacturer's instructions. Three images per well were taken and the % EdU positive cells and total number of cells were counted with ImageJ software (NIH). Three independent experiments were performed. A Student's T-test was used to determine significance (***$P < 0.001$, n = 3 [Brd4 siRNA])(*$P < 0.05$, n = 3 [48 h and 72 h 500 nM I-BET151 treatment]).

For **Figure S8**, U87MG cells were transfected with 25 nM of siRNA targeting *BRD2* (Ambion IDs66245), *BRD3* (Ambion, IDs15544) or *BRD4* (Ambion, IDs23901). Five days after transfection cells were treated with EdU as above. Counting of EdU-positive cells was performed with the Cellomix Array VTI Scan (Thermo Scientific) and the percentage of EdU positive cells was calculated with the Bio-application software "Target Activation" as ratio of nuclei to EdU-positive cells. For each sample, 25 fields were counted in order to cover the entire surface of the well.

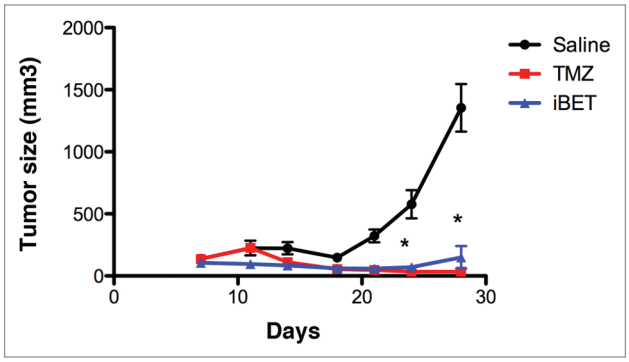

Figure 6. I-BET151 treatment reduces growth of U87MG cells in immunocompromised mice. I-BET151 (10 mg/kg, n = 8) or Saline (n = 9) was injected into NU-Foxn1nu mice that had been previously injected with U87MG cells. Eight mice were injected with I-BET151 and 9 mice were injected with saline. Tumor sizes were measured every two to three days using caliper measurements. Average and standard deviation per day are shown. Average and standard error of the mean per day are shown for mice independently injected and analyzed.

Propidium Iodide-FACS

An amount of 1×10^5 U87MG cells were plated into two wells of a six well plate. Twenty-four hours later, 500nM of I-BET151 or DMSO was added to each well and processed for PI-FACS as previously described.[29] GraphPad prism was used to analyze the FACS data. Two-way ANOVA was used to determine significance (****$P < 0.0001$, n = 3).

Fluorescence ubiquitination cell cycle indicator (FUCCI) analysis

U87MG cells were plated at a low confluency (25–30%) and transduced with geminin-GFP and Cdt1-RFP expressing virus (Premo™ FUCCI Cell Cycle Sensor BacMam 2.0, Invitrogen) for 16 h following the manufacturer's instructions. These two constructs are ubiquitinated by specific ubiquitin E3 ligases targeting them to the proteasome for degradation. These E3 ligases are temporarily regulated during the cell cycle. As a result, the nuclei of the cells progressing through the cell cycle varied in color: the nuclei of cells in G1 phase were labeled with the red fluorescent protein (RFP). The nuclei of cells in S through M phases were labeled with the green fluorescent protein (GFP). As the cells transitioned between phases G1 and S, they expressed both RFP and GFP, appearing yellow after image co-localization. Cells lacking color were transitioning between M and G1.

Media containing 500 nM I-BET151 or DMSO was added to the transduced cells. Cells were then immediately placed in a microscope incubator chamber and images were captured every hour for 24 h (Confocal LSM7, Leica). Time series images were analyzed with the Fiji software obtaining the number of cells in each cell cycle phase. Three independent experiments were performed. Using GraphPad Prism, data were analyzed by Two-way repeated measures ANOVA, followed by Bonferroni

Post hoc comparison of all the means to determine significance (***$P < 0.001$; **$P < 0.01$; *$P < 0.05$; n = 3).

Compounds

I-BET151 (GSK1210151A) was synthesized to > 99.5% purity as described in Dawson et al.[3] by Reagents 4 Research LLC. Temozolomide was purchased from Tocris Bioscience (Catalog Number 2706). BKM-120 (Catalog Number S2247), GDC-0941 (S1065), MLN8237 (S1133), MK-2206 (S1078), and PD0332991 were purchased from SelleckChem.

BRD2, BRD3 and BRD4 knockdown

U87MG cells were plated and transfected the same day with Lipofectamine (Life Technologies) and 50 nM siRNA (Silencer Select validated siRNA for BRD4 ID#s23901 and Negative Control ID#4390843) according to the manufacturer's instructions. Cells were transfected a second time 2 d after plating and RNA extracted 5 d after plating. U87MG were transfected with 25 nM of siRNAs targeting either BRD2 (IDs66245) or BRD3 (IDs15544). Cells were then lysed with Trizol (Life Technologies), total RNA extracted with chloroform, and the RNA was further purified with the RNeasy Mini Kit (Qiagen). cDNA was synthesized (cat#18080-400, Life Technologies) and real-time qPCR performed with Taqman probes for BRD4 or actin. The amount of target gene expression was calculated in relation to a reference gene using ΔΔCt analysis ($2^{-[0Ct\ target-Ct\ reference]}$). Error bars represent the standard deviation from the mean for three independent experiments (***$P < 0.001$ as determined by the Student *t* test; n = 3).

UM20 cell line

Glioblastoma tissue was washed with PBS, minced, and incubated in 0.1% trypsin and 0.04% DNase in Hank's balanced salt solution (HBSS) for 45 min at 37 °C while rotating. Cells were then passed through a 70 μm and 40μm filter and plated. They were grown as a monolayer in DMEM/F12 (1:1) containing non-essential amino acids (NEAA) supplemented with 5% FBS.

Patient derived GBM stem cells (Glio1 and Glio3)

Tumors were minced in PBS and digested in Hanks balanced salt solution (HBSS) containing 0.1% trypsin/EDTA and 0.2 mg/ml DNase I (Roche) for 30 min at 37 °C. Cells were serially passed through 70 then 40 μm filters, pelleted and incubated with red cell lysis buffer (Sigma) to remove red blood cells. Cells were washed in DMEM and plated in DMEM/F12 (3:1) (Life Technologies) supplemented with 20 ng/ml EGF, 20 ng/ml bFGF, and 2% Gem21Neuroplex and 1% anti-mycotic/anti-biotic (Gemini Bio-Products; 300-110P, 300-112P, 400161-010, 400101). Neurospheres were dissociated with Accutase (Invitrogen; A1110501) and one-half of the media was replaced twice a week. Neurospheres were fixed in 4% paraformaldehyde, blocked in 5% BSA with 0.6% triton X-100 for 1 h and incubated with CD133 and nestin, (Abcam; ab19898, ab6320;) overnight. Following 1 h incubation with secondary antibodies (Molecular Probes), nuclei were labeled with DAPI and cells were visualized with fluorescence microscopy. For western blot analysis, neurosphere cells were lysed in ice-cold RIPA buffer (1% sodium deoxycholate, 0.1% SDS, 1% triton-X-100, 10 mM Tris pH 8, 140 mM NaCl) supplemented with 250 units/ml benzonase, 1 mM dithiothreitol (DTT), and phosSTOP phosphatase inhibitor cocktail and Complete protease inhibitor cocktail both obtained from Roche (04906837001, 05892791001). Proteins (20 μg) were run on 8 and 12% acrylamide gels, transferred to nitrocellulose and probed with nestin, cleaved notch1, (Abcam; ab6320, ab52301) musashi (Cell Signaling Technology; 5663) and β-actin (Millipore; MAB1501).

I-BET151 treatment of xenografted U87MG Cells

U87MG cells were grown to 70–80% confluency, washed with PBS, trypsinized, counted, and re-suspended in Advanced DMEM/F12 (Invitrogen, cat# 12634) at a concentration of 15×10^6 per mL. NU-Foxn1nu mice (Charles River Laboratories [n = 17] were injected subcutaneously in the right flank with 200 μl of the cell solution (3×10^6 cells per mouse). Mice were weighed once a week. Tumor sizes were measured with digital calipers every two to three days, recorded, and used for tumor volume calculations (WxLxH). Treatment with I-BET151 began 7 d after subcutaneous injection. The mice were evenly grouped with reference to tumor volume at the beginning of treatment. Eight mice were injected with I-BET151 and nine mice were injected with saline. I-BET151 was dissolved in 5% Tween80 (Sigma-Aldrich, cat# P1754, 500 mL), 5% DMSO (Sigma-Aldrich, cat# 34869), and 90% saline (G Biosciences, cat# 786-561). Intraperitoneal injections (IP) were administered daily at a concentration of 10 mg/kg for 21 d.

Array gene ST

U87MG, A172, T98G, LN18, Patient Glioblastoma Stem Cell 1 (Glio1), Patient Glioblastoma Stem Cell 3 (Glio3) were plated and subsequently treated with DMSO or I-BET151 at a concentration of 500 nM for 24h. RNA was extracted (Qiagen kit), cDNA synthesized (Life technology), and hybridized to Affymetrix Gene 1.0 ST as previously described.[29]

Array data analysis

The Human Gene ST 1.0 array interrogates 36,079 annotated RefSeq (build 36) transcripts (Gene ST 2.0 covers 40,716 transcripts RefSeq build 51). The probe set intensities were quantified using the Affymetrix Scanners using GeneChip Command Console (AGCC) and analyzed with RMA normalization using Genome Console software (Affymetrix).

Disclosure of Potential Conflicts of Interest

No potential conflicts of interest were disclosed.

Funding

This work was supported by R01NS067289 to Nagi Ayad. Regina M. Graham is supported by the Mystic Force Foundation. Dr.Sarkaria is supported by Mayo Brain Tumor SPORE CA108961 and RO1 CA176830.

Acknowledgments

We thank all members of the Center for Therapeutic Innovation for helpful discussions and suggestions. We thank the Cell Based Screening Core at Scripps Florida and the Oncogenomics Core at The University of Miami. We thank Amade Bregy and Ashish Shah for their help and coordination of tumor samples. We thank Jeff Albert for sharing unpublished results regarding PK properties of I-BET151. R.M.G. is supported by the Mystic Force

Foundation. J.N.S. is supported by Mayo Brain Tumor SPORE CA108961 and RO1 CA176830.

Supplemental Materials

Supplemental materials may be found here:
www.landesbioscience.com/journals/epigenetics/article/27906

References

1. Dawson MA, Kouzarides T. Cancer epigenetics: from mechanism to therapy. Cell 2012; 150:12-27; PMID:22770212; http://dx.doi.org/10.1016/j.cell.2012.06.013
2. Dawson MA, Kouzarides T, Huntly BJ. Targeting epigenetic readers in cancer. N Engl J Med 2012; 367:647-57; PMID:22894577; http://dx.doi.org/10.1056/NEJMra1112635
3. Dawson MA, Prinjha RK, Dittmann A, Giotopoulos G, Bantscheff M, Chan WI, Robson SC, Chung CW, Hopf C, Savitski MM, et al. Inhibition of BET recruitment to chromatin as an effective treatment for MLL-fusion leukaemia. Nature 2011; 478:529-33; PMID:21964340; http://dx.doi.org/10.1038/nature10509
4. Yang Z, Yik JH, Chen R, He N, Jang MK, Ozato K, Zhou Q. Recruitment of P-TEFb for stimulation of transcriptional elongation by the bromodomain protein Brd4. Mol Cell 2005; 19:535-45; PMID:16109377; http://dx.doi.org/10.1016/j.molcel.2005.06.029
5. Yang XJ. Multisite protein modification and intramolecular signaling. Oncogene 2005; 24:1653-62; PMID:15744326; http://dx.doi.org/10.1038/sj.onc.1208173
6. Filippakopoulos P, Qi J, Picaud S, Shen Y, Smith WB, Fedorov O, Morse EM, Keates T, Hickman TT, Felletar I, et al. Selective inhibition of BET bromodomains. Nature 2010; 468:1067-73; PMID:20871596; http://dx.doi.org/10.1038/nature09504
7. Nicodeme E, Jeffrey KL, Schaefer U, Beinke S, Dewell S, Chung CW, Chandwani R, Marazzi I, Wilson P, Coste H, et al. Suppression of inflammation by a synthetic histone mimic. Nature 2010; 468:1119-23; PMID:21068722; http://dx.doi.org/10.1038/nature09589
8. Zuber J, Shi J, Wang E, Rappaport AR, Herrmann H, Sison EA, Magoon D, Qi J, Blatt K, Wunderlich M, et al. RNAi screen identifies Brd4 as a therapeutic target in acute myeloid leukaemia. Nature 2011; 478:524-8; PMID:21814200; http://dx.doi.org/10.1038/nature10334
9. Delmore JE, Issa GC, Lemieux ME, Rahl PB, Shi J, Jacobs HM, Kastritis E, Gilpatrick T, Paranal RM, Qi J, et al. BET bromodomain inhibition as a therapeutic strategy to target c-Myc. Cell 2011; 146:904-17; PMID:21889194; http://dx.doi.org/10.1016/j.cell.2011.08.017
10. Belkina AC, Blanton WP, Nikolajczyk BS, Denis GV. The double bromodomain protein Brd2 promotes B cell expansion and mitogenesis. J Leukoc Biol 2013; Forthcoming; PMID:24319289; http://dx.doi.org/10.1189/jlb.1112588
11. Ott CJ, Kopp N, Bird L, Paranal RM, Qi J, Bowman T, Rodig SJ, Kung AL, Bradner JE, Weinstock DM. BET bromodomain inhibition targets both c-Myc and IL7R in high-risk acute lymphoblastic leukemia. Blood 2012; 120:2843-52; PMID:22904298; http://dx.doi.org/10.1182/blood-2012-02-413021
12. Belkina AC, Nikolajczyk BS, Denis GV. BET protein function is required for inflammation: Brd2 genetic disruption and BET inhibitor JQ1 impair mouse macrophage inflammatory responses. J Immunol 2013; 190:3670-8; PMID:23420887; http://dx.doi.org/10.4049/jimmunol.1202838
13. Stupp R, Hegi ME, Mason WP, van den Bent MJ, Taphoorn MJ, Janzer RC, Ludwin SK, Allgeier A, Fisher B, Belanger K, et al.; European Organisation for Research and Treatment of Cancer Brain Tumour and Radiation Oncology Groups; National Cancer Institute of Canada Clinical Trials Group. Effects of radiotherapy with concomitant and adjuvant temozolomide versus radiotherapy alone on survival in glioblastoma in a randomised phase III study: 5-year analysis of the EORTC-NCIC trial. Lancet Oncol 2009; 10:459-66; PMID:19269895; http://dx.doi.org/10.1016/S1470-2045(09)70025-7
14. Lacroix M, Abi-Said D, Fourney DR, Gokaslan ZL, Shi W, DeMonte F, Lang FF, McCutcheon IE, Hassenbusch SJ, Holland E, et al. A multivariate analysis of 416 patients with glioblastoma multiforme: prognosis, extent of resection, and survival. J Neurosurg 2001; 95:190-8; PMID:11780887; http://dx.doi.org/10.3171/jns.2001.95.2.0190
15. Chen J, Li Y, Yu TS, McKay RM, Burns DK, Kernie SG, Parada LF. A restricted cell population propagates glioblastoma growth after chemotherapy. Nature 2012; 488:522-6; PMID:22854781; http://dx.doi.org/10.1038/nature11287
16. Geiss GK, Bumgarner RE, Birditt B, Dahl T, Dowidar N, Dunaway DL, Fell HP, Ferree S, George RD, Grogan T, et al. Direct multiplexed measurement of gene expression with color-coded probe pairs. Nat Biotechnol 2008; 26:317-25; PMID:18278033; http://dx.doi.org/10.1038/nbt1385
17. Benjamini YaH. Y. Controlling the False Discovery Rate: a Practical and Powerful Approach to Multiple Testing. J R Stat Soc, B 1995; 57:289-300
18. Sakaue-Sawano A, Kurokawa H, Morimura T, Hanyu A, Hama H, Osawa H, Kashiwagi S, Fukami K, Miyata T, Miyoshi H, et al. Visualizing spatiotemporal dynamics of multicellular cell-cycle progression. Cell 2008; 132:487-98; PMID:18267078; http://dx.doi.org/10.1016/j.cell.2007.12.033
19. Seal J, Lamotte Y, Donche F, Bouillot A, Mirguet O, Gellibert F, Nicodeme E, Krysa G, Kirilovsky J, Beinke S, et al. Identification of a novel series of BET family bromodomain inhibitors: binding mode and profile of I-BET151 (GSK1210151A). Bioorg Med Chem Lett 2012; 22:2968-72; PMID:22437115; http://dx.doi.org/10.1016/j.bmcl.2012.02.041
20. Greenwald RJ, Tumang JR, Sinha A, Currier N, Cardiff RD, Rothstein TL, Faller DV, Denis GV. E mu-BRD2 transgenic mice develop B-cell lymphoma and leukemia. Blood 2004; 103:1475-84; PMID:14563639; http://dx.doi.org/10.1182/blood-2003-06-2116
21. Sinha A, Faller DV, Denis GV. Bromodomain analysis of Brd2-dependent transcriptional activation of cyclin A. Biochem J 2005; 387:257-69; PMID:15548137; http://dx.doi.org/10.1042/BJ20041793
22. Cheng Z, Gong Y, Ma Y, Lu K, Lu X, Pierce LA, Thompson RC, Muller S, Knapp S, Wang J. Inhibition of BET bromodomain targets genetically diverse glioblastoma. Clin Cancer Res 2013; 19:1748-59; PMID:23403638; http://dx.doi.org/10.1158/1078-0432.CCR-12-3066
23. Wang H, Shimizu E, Tang YP, Cho M, Kyin M, Zuo W, Robinson DA, Alaimo PJ, Zhang C, Morimoto H, et al. Inducible protein knockout reveals temporal requirement of CaMKII reactivation for memory consolidation in the brain. Proc Natl Acad Sci U S A 2003; 100:4287-92; PMID:12646704; http://dx.doi.org/10.1073/pnas.0636870100
24. Merrick KA, Wohlbold L, Zhang C, Allen JJ, Horiuchi D, Huskey NE, Goga A, Shokat KM, Fisher RP. Switching Cdk2 on or off with small molecules to reveal requirements in human cell proliferation. Mol Cell 2011; 42:624-36; PMID:21658603; http://dx.doi.org/10.1016/j.molcel.2011.03.031
25. Lovén J, Hoke HA, Lin CY, Lau A, Orlando DA, Vakoc CR, Bradner JE, Lee TI, Young RA. Selective inhibition of tumor oncogenes by disruption of super-enhancers. Cell 2013; 153:320-34; PMID:23582323; http://dx.doi.org/10.1016/j.cell.2013.03.036
26. Banerjee C, Archin N, Michaels D, Belkina AC, Denis GV, Bradner J, Sebastiani P, Margolis DM, Montano M. BET bromodomain inhibition as a novel strategy for reactivation of HIV-1. J Leukoc Biol 2012; 92:1147-54; PMID:22802445; http://dx.doi.org/10.1189/jlb.0312165
27. Clarke J, Penas C, Pastori C, Komotar RJ, Bregy A, Shah AH, Wahlestedt C, Ayad NG. Epigenetic pathways and glioblastoma treatment. Epigenetics 2013; 8:785-95; PMID:23807265; http://dx.doi.org/10.4161/epi.25440
28. Carlson BL, Pokorny JL, Schroeder MA, Sarkaria JN. Establishment, maintenance and in vitro and in vivo applications of primary human glioblastoma multiforme (GBM) xenograft models for translational biology studies and drug discovery. Curr Protoc Pharmacol 2011; Chapter 14:Unit 14 6.
29. Smith A, Simanski S, Fallahi M, Ayad NG. Redundant ubiquitin ligase activities regulate wee1 degradation and mitotic entry. Cell Cycle 2007; 6:2795-9; PMID:18032919; http://dx.doi.org/10.4161/cc.6.22.4919
30. Liu L, Zhen XT, Denton E, Marsden BD, Schapira M. ChromoHub: a data hub for navigators of chromatin-mediated signalling. Bioinformatics 2012; 28:2205-6; PMID:22718786; http://dx.doi.org/10.1093/bioinformatics/bts340